

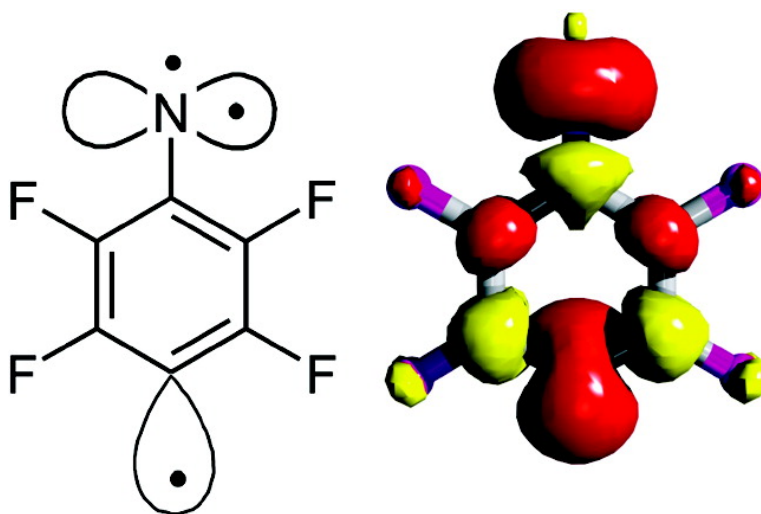
Article

2,3,5,6-Tetrafluorophenylnitren-4-yl: Electron Paramagnetic Resonance Spectroscopic Characterization of a Quartet-Ground-State Nitreno Radical

Wolfram Sander, Dirk Grote, Simone Kossmann, and Frank Neese

J. Am. Chem. Soc., **2008**, 130 (13), 4396-4403 • DOI: 10.1021/ja078171s

Downloaded from <http://pubs.acs.org> on February 8, 2009



More About This Article

Additional resources and features associated with this article are available within the HTML version:

- Supporting Information
- Links to the 1 articles that cite this article, as of the time of this article download
- Access to high resolution figures
- Links to articles and content related to this article
- Copyright permission to reproduce figures and/or text from this article

[View the Full Text HTML](#)



ACS Publications
 High quality. High impact.

2,3,5,6-Tetrafluorophenylnitren-4-yl: Electron Paramagnetic Resonance Spectroscopic Characterization of a Quartet-Ground-State Nitreno Radical

Wolfram Sander,^{*,†} Dirk Grote,[†] Simone Kossmann,[‡] and Frank Neese^{*,‡}

*Lehrstuhl für Organische Chemie II, Ruhr-Universität Bochum, D-44780 Bochum, Germany, and
Lehrstuhl für Theoretische Chemie, Universität Bonn, D-53115 Bonn, Germany*

Received October 25, 2007; E-mail: wolfram.sander@rub.de

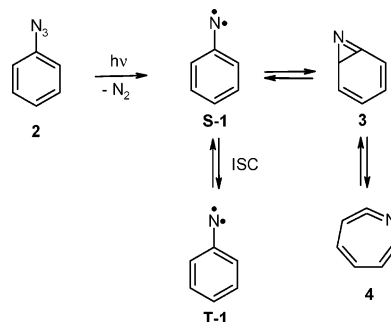
Abstract: 2,3,5,6-Tetrafluorophenylnitren-4-yl (**5**) was synthesized in argon at 4 K via the photolysis of 2,3,5,6-tetrafluoro-4-iodo-phenyl azide (**6**). Electron paramagnetic resonance (EPR) spectroscopy allows us to observe triradical **5** in its quartet state with the zero-field splitting (ZFS) parameters $|D/hc| = 0.285$ and $|E/hc| = 0.043$ cm⁻¹. The quartet ground state of **5** is in accordance with our previous infrared (IR) spectroscopic investigation, in which the high-spin quartet state, but no low-spin doublet state, of **5** was observed in solid argon at 4 K [Wenk, H. H.; Sander, W. *Angew. Chem., Int. Ed.* **2002**, *41*, 2742–2745]. Because annealing of the matrix at temperatures of >10 K results in the rapid recombination of the highly reactive species **5** with I atoms produced during the photolysis of **6**, the Curie–Weiss behavior could not be investigated. However, the absence of low-spin states in the IR investigations, as well as the results of ab initio and density functional theory (DFT) calculations, strongly suggest that **5** has a robust quartet ground state that is best-described as an unprecedented σ,σ,π -triradical. The ZFS of **5** has been successfully reproduced by DFT calculations, which furthermore provide qualitative insight into the origin of the observed EPR parameters.

Introduction

Arylnitrenes (**1**; see Scheme 1) are important reactive intermediates with triplet ground states and large singlet triplet splittings. Convenient precursors for spectroscopic studies are the corresponding aryl azides **2**, which photochemically or thermally split off N₂ to produce the nitrenes **1**. The kinetics, spectroscopy, and computational chemistry of these intermediates has recently been reviewed.¹ Under the conditions of matrix isolation a major photochemical process that diminishes the yield of nitrenes **1** is the ring expansion to 1,2-didehydroazepines **4**, via benzazirines **3** as intermediates. After many years of intense experimental and theoretical work in this field, the mechanistic details are now well established (see Scheme 1).

The introduction of a radical center in *para* position of the phenyl ring leads to phenylnitreno radicals, which represent a new class of reactive intermediates.^{2–4} The first example of these intermediates that could be isolated in low-temperature matrices is 2,3,5,6-tetrafluorophenylnitren-4-yl **5**.² Ultraviolet (UV) photolysis (254 nm) of aryl azide **6**, matrix-isolated in argon at 4 K, produced nitrene **7** that could be easily identified by comparison of the experimental infrared (IR) spectrum with

Scheme 1. Mechanism of the Rearrangement of Phenylnitrene **1**



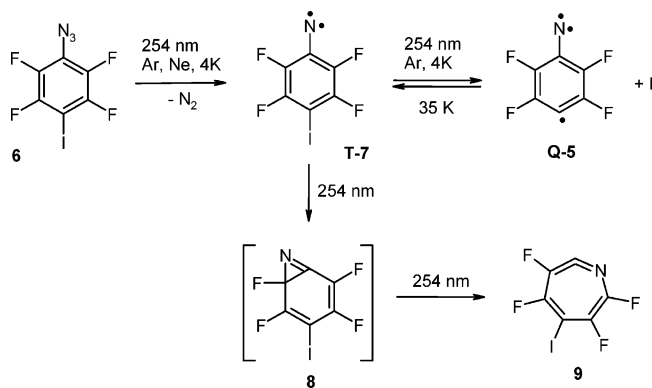
density functional theory (DFT) calculations (UB3LYP/6-311G-(d,p)). Further UV irradiation resulted in the formation of two new products: ketenimine (**9**) (presumably formed via azirine (**8**) that could not be detected) and nitreno radical **5** (see Scheme 2). The radical **5** was only observed if the matrix was kept at a temperature of 3–4 K during irradiation, whereas at 10 K, only traces of **5** were formed. The formation of **5** is reversible, and annealing the matrix resulted in recombination with the I atom to yield nitrene **7**. This explains why the nitreno radical **5** was only observed at temperatures of <10 K.

The IR spectra calculated for the lowest-lying doublet state **D-5** and quartet state **Q-5** exhibit characteristic differences that allowed these two states to be differentiated by IR spectroscopy. The IR spectrum of matrix-isolated **5** was in good agreement with that calculated for **Q-5**, whereas **D-5** was not

[†] Ruhr-Universität Bochum.

[‡] Universität Bonn.

(1) Gritsan, N. P.; Platz, M. S. *Chem. Rev.* **2006**, *106*, 3844–3867.
(2) Wenk, H. H.; Sander, W. *Angew. Chem., Int. Ed.* **2002**, *41*, 2742–2745.
(3) Bettinger, H. F.; Sander, W. *J. Am. Chem. Soc.* **2003**, *125*, 9726–9733.
(4) Sander, W.; Winkler, M.; Cakir, B.; Grote, D.; Bettinger, H. F. *J. Org. Chem.* **2007**, *72*, 715–724.

Scheme 2. Photochemistry of Aryl Azide (**6**)

observed.² This suggests a quartet ground state of **5**, in accordance with the results from a theoretical study, which predict quartet ground states for aryl nitreno radicals if the radical center is in the ortho or para position of the phenyl ring, whereas a radical center in the meta position should result in a doublet ground state.³ Attempts to synthesize *meta*-aryl nitreno radicals to verify the latter assumption failed, because these systems easily ring-open to thermally preferred nitriles.⁴

Results and Discussion

EPR Spectrum of T-7. An argon matrix doped with small amounts of aryl azide **6** was deposited on top of a copper rod that was maintained at 4 K. The copper rod was then positioned inside a quartz tube (within the high-vacuum system), which allowed the matrix-isolated azide **6** to be irradiated with a XeCl excimer laser (308 nm) and EPR spectra (X-band spectrometer) of the photoproducts to be recorded. After irradiation with a few laser pulses, three strong signals appear in the area between 7000 and 8500 G, which are assigned to the *x*2, *y*2, and *z*1 transitions of triplet nitrene **T-7**. A simulated EPR spectrum with the parameters $g = 2.003$, $|D/hc| = 1.108 \text{ cm}^{-1}$, and $|E/hc| = 0.012 \text{ cm}^{-1}$, assuming randomly oriented molecules, nicely reproduces the experimental spectrum. The large zero-field splitting (ZFS) parameter D is characteristic of triplet aryl nitrenes, which generally show values in the range of 0.8–1.1 cm^{-1} , depending on the substituents.⁵ The splitting of the *x*- and *y*-signals in the EPR spectrum of **T-7** of ~ 600 G corresponds to a ZFS parameter $|E/hc|$ of 0.012 cm^{-1} , which is larger than that in most aryl nitrenes. Thus, phenylnitrene ($|D/hc| = 0.9978 \text{ cm}^{-1}$, $|E/hc| < 0.002 \text{ cm}^{-1}$)⁵ and 2,3,5,6-tetrafluorophenylnitrene ($|D/hc| = 1.051 \text{ cm}^{-1}$, $|E/hc| = 0.0008 \text{ cm}^{-1}$) show E values that are close to zero. This indicates a significant influence of the iodine substituent on the ZFS parameters of **T-7**. Hall et al. investigated several 4-substituted phenyl nitrenes in methylcyclohexane at 77 K and observed, compared to the remainder of the investigated derivatives, a very broad EPR spectrum for 4-iodophenylnitrene.⁶ This was attributed to hyperfine coupling (HFC) with the iodine substituent. In our experiments in argon matrices, no HFC was observed, but a very well-resolved splitting between transitions *x*2 and *y*2 was observed. It is well-known that not only spin–spin dipolar interactions contribute to the ZFS parameters, but also spin–orbit effects.^{7,8} Because iodine (I) is a heavy atom,

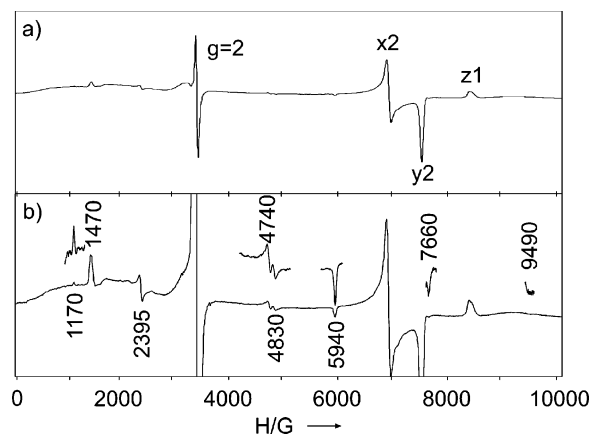


Figure 1. Electron paramagnetic resonance (EPR) spectra (9.5877 GHz) produced by 308-nm irradiation of arylazide (**6**), matrix-isolated in argon at 4 K: (a) spectrum obtained after short-time irradiation is dominated by unspecified radicals and triplet nitrene (**T-7**) with $|D/hc| = 1.108 \text{ cm}^{-1}$ and $|E/hc| = 0.012 \text{ cm}^{-1}$ ($g = 2.003$); (b) same matrix after prolonged irradiation. Several new signals are assigned to quartet nitreno radical (**Q-5**).

a significant contribution of spin–orbit coupling (SOC) to the ZFS parameters of **T-7** is very likely. This notion is also consistent with our preliminary calculations.

To obtain more insight into the effect of the halide substituent in the para position on the ZFS, calculations were performed for models ³⁷X with X = H, F, Cl, Br, I. Using B3LYP/TZVPP, the D value for ³⁷H is calculated to be 0.978 cm^{-1} with $E/D = 0.0074$. This value is well within the range typically observed for aromatic nitrenes. Changing the para-substituent from H to F leads to a moderate increase of the value of D (to 0.993) while the value of E/D decreases by a factor of ~ 2 (to 0.003). This is attributed to the higher symmetry of the system, compared to that of ³⁷H. On the other hand, replacement of F by Cl yields $D = 1.048$ and an increased E/D value of 0.056. Unfortunately, for the heavier halides (Br and I), we apparently face a breakdown of perturbation theory and the calculations provide unrealistic values for the ZFS. Hence, we have focused our attention on ³⁷Cl, where no problems are apparent. In this compound, the spin–spin interaction accounts for 0.882 cm^{-1} of D while the spin–orbit contribution already amounts to 0.227 cm^{-1} , which is a factor of ~ 2 larger than the SOC contribution in ³⁷H. In fact, practically all of the increase in the E/D values between ³⁷H and ³⁷Cl results from the spin–orbit contribution. This is readily rationalized by the mechanisms that govern the ZFS. For the spin–spin contribution, it will be explained in detail below that the principal axis points along the C–N bond. However, for the SOC contribution, the easy axis is perpendicular to the C–N bond and the plane of the molecule. Hence, after adding the spin–spin and spin–orbit contributions together, increased rhombicity will result.

EPR Spectrum of Q-5. Prolonged irradiation with the XeCl excimer laser (308 nm) at 4 K leads to new EPR signals at 1170, 1470, 2395, 4740, 4830, 5940, 7660, and 9490 G which continuously grow during the photolysis (Figure 1). When annealed at 30 K, these signals disappear but can be recovered when subjected to 308 nm irradiation at 4 K. This is characteristic behavior of radical pairs produced by the photolysis of

(5) Wasserman, E. *Prog. Phys. Org. Chem.* **1971**, *8*, 319–336.

(6) Hall, J. H.; Fargher, J. M.; Gislser, M. R. *J. Am. Chem. Soc.* **1978**, *100*, 2029–2034.

(7) Glarum, S. H. *J. Chem. Phys.* **1963**, *39*, 3141–3144.

(8) Weltner, W., Jr.; Van Zee, R. J.; Li, S. *J. Phys. Chem.* **1995**, *99*, 6277–6285.

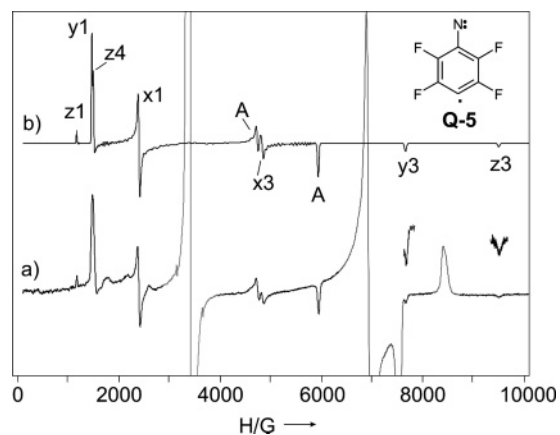


Figure 2. (a) EPR spectrum (9.5875 GHz) of **Q-5** in solid argon at 4 K produced by 308 nm irradiation of **6**. (b) Simulation of the spectrum of **Q-5** using the following parameters: $g = 2.003$, $|D/hc| = 0.285 \text{ cm}^{-1}$ and $|E/hc| = 0.043 \text{ cm}^{-1}$.

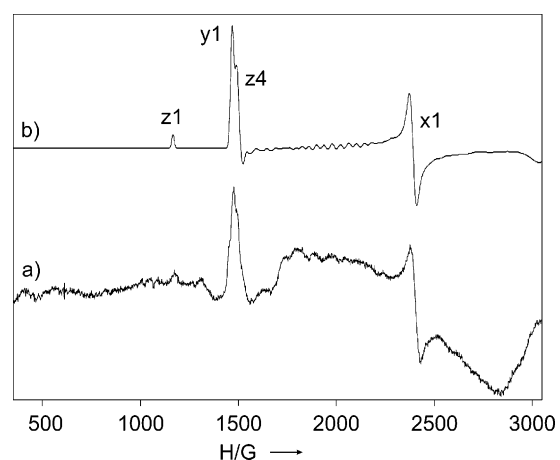


Figure 3. Low field area showing details of the EPR spectrum (9.5752 GHz) of **Q-5**: (a) experimental spectrum and (b) simulated spectrum. The shape of the signals was adapted to match the experimental spectrum.

matrix-isolated precursors. The radical pair is formed in close proximity in the matrix, and annealing leads to rapid recombination. This is exactly the same behavior previously observed for **Q-5** and I atoms, using IR detection;² thus, the labile signals are assigned to the nitrene radical in its quartet ground state. The I atoms formed during photolysis could not be observed in the electron spin resonance (ESR) spectra. This has been also found in other experiments and is attributed to the orbital degeneracy and strong spin-orbit coupling in the I atoms, resulting in very broad signals. EPR spectra of matrix-isolated I atoms were only observed in solid xenon and other matrices with stronger interactions between I atoms and the matrix.^{9,10}

Simulation of the EPR Spectrum. The simulation of the EPR spectrum of **Q-5** with ZFS parameters $|D/hc| = 0.285$ and $|E/hc| = 0.043 \text{ cm}^{-1}$ resulted in excellent agreement with the experimental spectrum (see Figures 2 and 3). The assignment of the transitions (given in Table 1) is based on the simulated

Table 1. Assignment of the EPR Transitions of **Q-5**

Signal		experiment	transition	assignment
simulation	calculation			
1165	1165	1170	$z, 1\rangle \leftrightarrow 2\rangle$	z1
1470	1465	1465	$y, 3\rangle \leftrightarrow 4\rangle$	y1
1490	1525	1480	$z, 2\rangle \leftrightarrow 4\rangle$	z4
2395	2390	2395	$x, 3\rangle \leftrightarrow 4\rangle$	x1
	4125		$z, 2\rangle \leftrightarrow 4\rangle$	z4'
4725		4740		A
4825	4810	4830	$x, 1\rangle \leftrightarrow 2\rangle$	x3
5935		5940		A
7655	7620	7660	$y, 1\rangle \leftrightarrow 2\rangle$	y3
9495	9450	9490	$z, 3\rangle \leftrightarrow 4\rangle$	z3

spectrum. The field dependence of the magnetic energy levels was calculated for the principal axes, using the solution of the Hamilton matrix of a quartet state^{11,12} with the parameters derived from the simulation. The axial transitions for the external magnetic field parallel to the x -, y -, and z -direction, and their positions in the spectrum (depending on the ZFS parameters) are shown in Figures 4 and 5, respectively. Transition z4 appears in the spectrum if D is greater than $\sim 0.16 \text{ cm}^{-1}$ and moves with increasing D value to higher field values (see Figure 5).

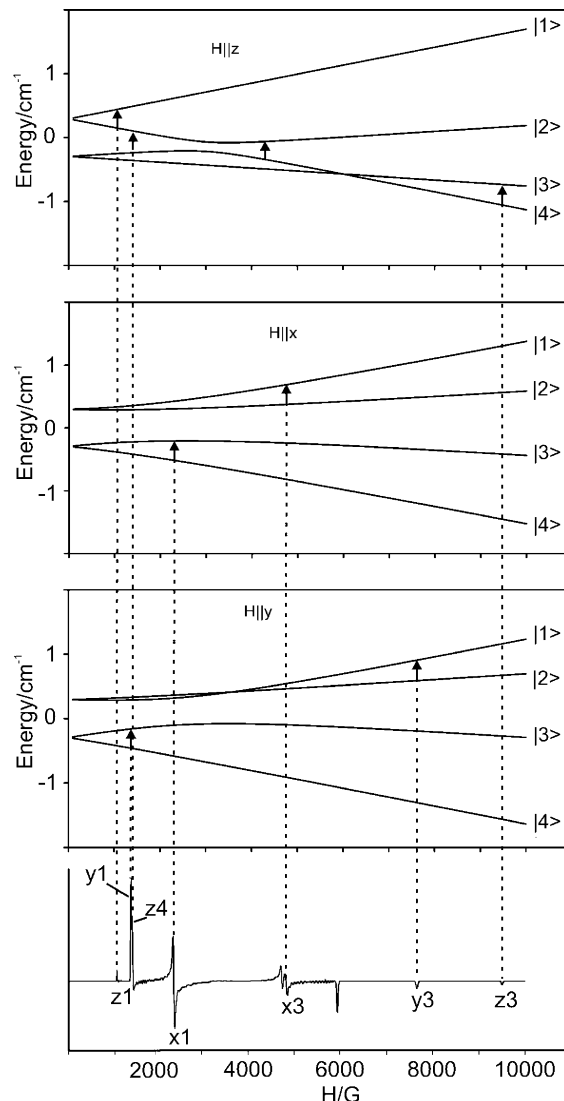


Figure 4. Energy of the four quartet sublevels, as a function of the external field H parallel to the z -, x - and y -axis, respectively, calculated for $|D/hc| = 0.285 \text{ cm}^{-1}$ and $|E/hc| = 0.043 \text{ cm}^{-1}$ ($g_{\text{iso}} = 2.003$).

- (9) Iwasaki, M.; Toriyama, K.; Muto, H. *J. Chem. Phys.* **1979**, *71*, 2853–2859.
 (10) Rai, U. S.; Symons, M. C. R.; Wyatt, J. L.; Bowman, W. R. *J. Chem. Soc., Faraday Trans.* **1993**, *89*, 1199–1201.
 (11) Atherton, N. M. *Principles of Electron Spin Resonance*; Prentice Hall: New York, 1993.
 (12) Fleischhauer, P.; Gehring, S.; Saal, C.; Haase, W.; Tomkowicz, Z.; Zanchini, C.; Gatteschi, D.; Davidov, D.; Barra, A. L. *J. Magn. Magn. Mater.* **1996**, *159*, 166–174.

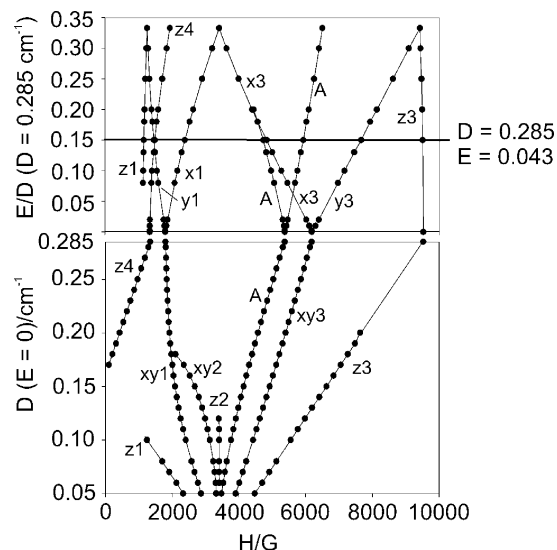


Figure 5. Simulation of the field dependence of the axial transitions of a quartet system with $D = 0.05\text{--}0.285\text{ cm}^{-1}$ and E/D values up to $1/3$. The signal positions of **5** with $|D/hc| = 0.285$ and $|E/hc| = 0.043\text{ cm}^{-1}$ are marked. Note that only the most intense signals were traced.

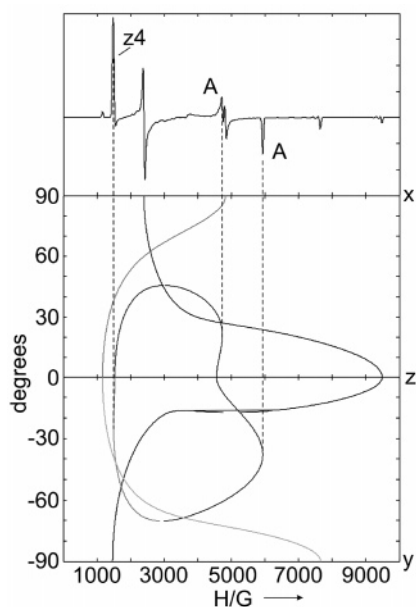


Figure 6. Angular dependence of the EPR signals of **Q-5** when varying the field orientation from parallel x to parallel z and parallel y . The signals marked as “A” can be assigned to off-axis transitions. The plot also shows the off-axis behavior of transition z_4 .

As for all z signals, the position of z_4 in the spectrum does not change significantly by changing the value of E , if D is constant. By contrast, the position of the x and y signals are very sensitive to changes in the value of E . The splitting between the corresponding x and y signals increases as the value of E increases, and, with an E/D ratio of $1/3$, the corresponding z and y signals, as well as the x_1 and x_3 signals, merge into one signal (see Figure 5). This behavior is known for triplet systems and confirms that the assignment of the transition (see Table 1) is consistent. In addition, there are two transitions A that are not assignable to axial transitions. (See Figure 6.) These transitions correspond to higher-order solutions of the spin Hamiltonian and are characteristic for high-spin systems ($S > 1$) with large ZFS parameters.^{13,14} Transition A, as well as

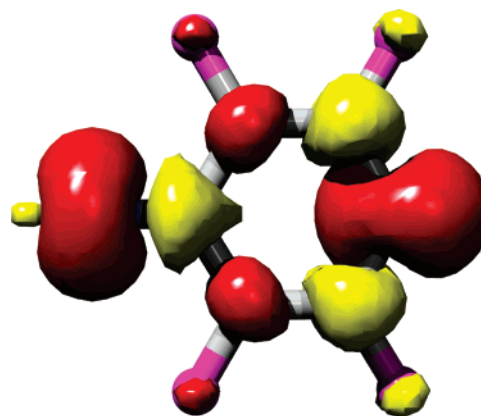
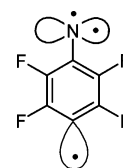


Figure 7. Spin-density distribution in **Q-5**. Positive values are contoured in red at the level of $0.003\text{ e}^-/(\text{Bohr}^3)$; negative values are contoured in yellow at a level of $-0.002\text{ e}^-/(\text{Bohr}^3)$.

transition z_4 , also split for $E > 0$; however, these signals do not merge with corresponding transitions at $E/D = 1/3$. This behavior is expected for off-axis transitions. Therefore, although transition z_4 can be assigned to an axial transition, it also exhibits some behavior that is characteristic of an off-axis transition. This z_4 is a transition between levels $|2\rangle$ and $|4\rangle$. According to the literature, such transitions are forbidden for $H \parallel z$, but become allowed if the z -axis is rotated away from the direction of the magnetic field.¹² This quasi off-axis nature of z_4 is also supported by the calculation of its angular dependence, and this might be the reason for the significant error of 35 G between the calculation and the simulation of this transition. Transitions y_1 and z_4 are predicted by the simulation to be very close at $\sim 1470\text{ G}$, and, indeed, a closer inspection of the experimental spectrum reveals a splitting of this peak into two components at 1465 and 1480 G.

Electronic Structure Calculations. The quartet ground state of **Q-5**, calculated with DFT, shows a fairly complex spin-density distribution, which involves π - as well as σ -components (Figure 7). More insight is obtained by identifying the singly occupied molecular orbitals (SOMOs) of the system. This is most conveniently done by examining the exactly singly occupied spin unrestricted natural orbitals (UNOs) transformed to a localized representation (Figure 8). The analysis suggests the following interpretation: The electronic structure of **Q-5** is best described as having two parallel-spin unpaired electrons localized on the nitrogen and one on the unsaturated carbon atom. The unpaired electron sitting in the in-plane nitrogen “lone pair” is fairly well-localized and only slightly polarizes the sigma-system of the ring. However, the unpaired electron sitting in the nitrogen out-of-plane lone pair is heavily delocalized into the π -system of the ring. Similarly, the carbon σ -lone pair is fairly delocalized into the σ -system of the ring. Schematically, the electronic structure may therefore be best-represented by the following leading resonance structure:



This is consistent with the notion that **Q-5** is best-described as a σ, σ, π -triradical.

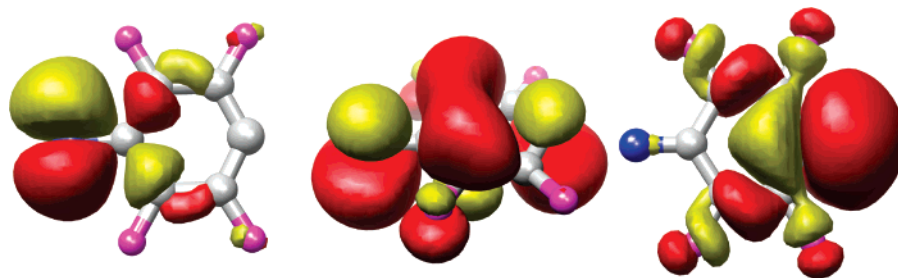


Figure 8. Three singly occupied molecular orbitals of **Q-5**: spin-unrestricted natural orbitals (UNOs) in a localized representation; Pipek–Mezey⁶⁰ localization; and B3LYP/TZVPP.

Ab initio calculations were performed to evaluate the extent to which **Q-5** indeed has an isolated quartet ground state. Because not all of the doublet states are properly represented by a single determinant, we resorted to correlated multireference ab initio methods in form of the spectroscopy-oriented configuration interaction (SORCI) approach,¹⁵ as implemented in the ORCA package.¹⁶ Calculations were performed on top of a state-averaged complete active space self-consistent field (SA-CASSCF) wavefunction for one quartet and two doublet states with three electrons in three orbitals. This constitutes the proper model space for answering the question raised previously. Starting orbitals were taken from the quasi-restricted orbitals (QROs)¹⁷ of a calculation with the BP^{18,19} function and the TZVPP²⁰ basis set (BP86/TZVPP). The active orbitals transform in the C_{2v} point group under the b_2 (in-plane nitrogen lone-pair), b_1 (out-of-plane nitrogen lone pair), and a_1 (carbon σ -lone pair) irreducible representations; hence, the lowest quartet state of the system is designated as 1^4A_2 .

The SORCI calculation was then performed on top of the SA-CASSCF(3,3) solution with $T_{\text{sel}} = 10^{-6}Eh$, $T_{\text{pre}} = 10^{-4}$, and $T_{\text{nat}} = 10^{-4}$ which provides essentially converged results for state energy differences.²¹ The calculations indeed predict 1^4A_2 to be the lowest state, followed by the first doublet (1^2A_2) at ~ 0.26 eV (6 kcal/mol) and the second doublet (2^2A_2) at ~ 0.95 eV (22 kcal/mol). Both low-lying doublet states are dominated by the same $(b_1)^1(b_2)^1(a_1)^1$ configuration that also applies to the 1^4A_2 ground state and correspond to the two linearly independent spin-doublet couplings that can be formed for three unpaired electrons in three orbitals. This result has two implications. First, it calls the spin-unrestricted Kohn–Sham solutions for the lowest doublet state (but not for the quartet state) into question, because it is not described well by a single determinant. Indeed, if no special care is taken, B3LYP^{18,22,23} DFT calculations predict the first doublet state to be ~ 0.7 eV above the ground state, which corresponds to an error of ~ 0.5 eV (~ 11 kcal/mol), relative to the more-reliable multireference ab initio calculation. Second, the quartet nature of the ground

Table 2. Analysis of the Calculated D -tensor (B3LYP/TZVPP) of **Q-5** (All Numbers Are Given in Units of cm^{-1})

	D	E
total (calc)	0.261	0.017
experiment	0.285	0.043
spin–spin	0.226	0.024
spin–orbit	0.035	−0.007
spin–spin		
1-center	0.273	0.034
2-center	−0.049	−0.010
3-center	0.002	0.000
4-center	0.000	0.000
coulomb	0.182	−0.018
exchange	0.044	0.042
spin–orbit		
$M = 0$ ($\alpha \rightarrow \alpha$)	−0.002	0.006
$M = 0$ ($\beta \rightarrow \beta$)	−0.001	0.006
$M = +1$ ($\beta \rightarrow \alpha$)	−0.001	−0.003
$M = -1$ ($\alpha \rightarrow \beta$)	0.040	−0.003

state becomes intelligible: The three SOMOs form an (accidentally) quasi-degenerate set (upon taking the ROHF solution of the 1^4A_2 state as a reference, the orbital energies are within < 2 eV of each other). Because the SOMOs are not well-separated spatially, the exchange interactions between the unpaired electrons must be large. Hence, the quartet state, which features the largest exchange stabilization, must be the ground state. These results show that, in agreement with the available experimental data, **Q-5** has a clear spin-quartet ground state and a strong preference for three unpaired electrons, even in the low-lying doublet states.

Calculations of the EPR Parameters. The EPR properties of **Q-5** (1^4A_2) were calculated with the B3LYP hybrid functional and a reasonably large TZVPP basis set, as described in the Experimental Section. The agreement between theory and experiment is very good for D , with respect to sign and magnitude, and is still reasonable for E (see Table 2). The near-perfect agreement observed for the value of D is, to some extent, certainly fortuitous; however, good agreement with the experiment is indeed anticipated from the results of Sinnecker and Neese.²⁴ The decomposition of D into individual contributions in Table 2 is interesting. Approximately 87% of D results from the direct spin–spin coupling (D^{SS}), and still $\sim 13\%$ comes from the SOC contribution. Interestingly, the calculated SS contribution is essentially local, with the largest contributions resulting from one-center integrals. Of the remaining contributions, the two-center terms reduce the local contributions by $\sim 18\%$, which

(13) Teki, Y.; Takui, T.; Yagi, H.; Itoh, K.; Iwamura, H. *J. Chem. Phys.* **1985**, *83*, 539–547.

(14) Matsushita, M.; Momose, T.; Shida, T.; Teki, Y.; Takui, T.; Itoh, K. *J. Am. Chem. Soc.* **1990**, *112*, 4700–4702.

(15) Neese, F. *J. Chem. Phys.* **2003**, *119*, 9428–9443.

(16) Neese, F. Version 2.6.04 ed.; University of Bonn, Germany, 2007.

(17) Neese, F. *J. Am. Chem. Soc.* **2006**, *128*, 10213–10222.

(18) Becke, A. D. *Phys. Rev. A* **1988**, *38*, 3098.

(19) Perdew, J. P. *Phys. Rev. B* **1986**, *33*, 8822–8824.

(20) Schäfer, A.; Huber, C.; Ahlrichs, R. *J. Chem. Phys.* **1994**, *100*, 5829.

(21) Wanko, M.; Hoffmann, M.; Strodel, P.; Thiel, W.; Neese, F.; Frauenheim, T.; Elstner, M. *J. Phys. Chem. B* **2005**, *109*, 3606–3615.

(22) Becke, A. D. *J. Chem. Phys.* **1993**, *98*, 1372–1377.

(23) Lee, C.; Yang, W.; Parr, R. G. *Phys. Rev. B: Condens. Matter Mater. Phys.* **1988**, *37*, 785–789.

(24) Sinnecker, S.; Neese, F. *J. Phys. Chem. A* **2006**, *110*, 12267–12275.

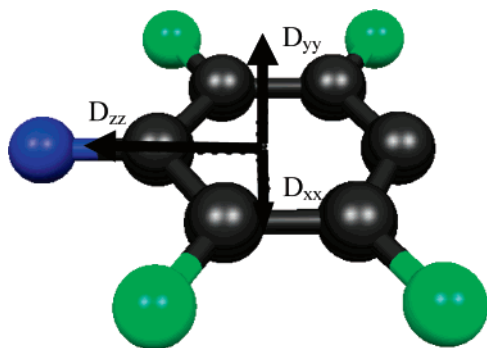


Figure 9. Orientation of the **D**-tensor of **Q-5**, based on the calculations (B3LYP/TZVPP).

emphasizes the importance of multicenter two-electron spin–spin integrals if quantitative agreement with the experiment is desired. The alternative breakdown of the SS term into Coulomb and exchange contributions shows that the latter are not negligible and possess the same sign as the Coulomb terms that are usually solely held responsible for the SS-term within a point dipole model. Indeed, the exchange terms, which, to the best of our knowledge, have rarely been discussed in the experimental EPR literature, account for $\sim 20\%$ of the SS term. This means that point dipole models are not realistic in the present systems; this is, of course, also consistent with the fact that the SS terms result from local one-center contributions, rather than from two-center Coulomb contributions as anticipated for a point dipole model.

The limited SOC contributions to D are dominated by the spin-lowering spin-flip contributions, which result from the low-lying spin-doublet states. This is consistent with previous results for other systems^{25–31} for which the SOC term represents the largest contribution to D . The SS contributions are calculated without any spin polarization. Unfortunately, it has been found previously that inclusion of spin polarization into the calculation of the SS term (which is technically feasible, of course) significantly degrades the agreement with the experimental values.²⁴ Thus, currently, there does not seem to be a satisfactory solution to this problem in a DFT framework.

Interestingly, the easy axis of the **D**-tensor does not point out of the plane but rather along the C–N bond (Figure 9). This result will be interpreted later in the Conclusions and Discussion section. The calculated g -shifts are -86.5 , 588 , and 1012 ppm. The small shifts are typical of radicals that are composed of light atoms. The orientation of the g -tensor is displayed graphically in Figure 10. Interestingly, the largest g -value—which also corresponds to the largest g -shift—is oriented perpendicular to the molecular plane and, therefore, also occurs perpendicular to the easy axis of the **D**-tensor. Nevertheless, the anisotropy in the g -tensor is sufficiently small, such that it is hardly possible to observe it under the present experimental conditions.

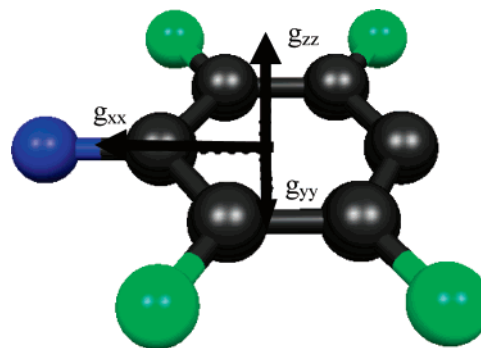
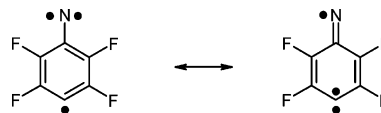


Figure 10. Orientation of the g -tensor of **Q-5**, based on the calculations (B3LYP/TZVPP).

Conclusions and Discussion

The EPR measurements confirm our previous assignments of the products of the matrix photolysis of **6**, based on IR spectroscopy.² As expected, the primary photoproduct is nitrene **T-7** formed in very high yield. The splitting of the C–I bond in **7** is much less efficient and competes with the rearrangement to **9**. Nevertheless, under conditions that allow the nitreno radical **5** to be detected via IR spectroscopy, a clear EPR signal of the quartet **Q-5** can be observed. It is pleasing that the previous assignment of the quartet state, based solely on IR spectroscopy, is now unequivocally confirmed by EPR spectroscopy. As observed in the IR experiments,² the yield of **5** is strongly dependent on the matrix temperature. At 10 – 15 K, only traces of **5** are formed, whereas the highest yield is found if **6** is irradiated at 4 K. Annealing at temperatures of >10 K results in the recombination of **5** with the I atom; therefore, it was not possible to measure the Curie–Weiss behavior of **5**.

The electronic structure of **Q-5** can be best-described as a σ,σ,π -triradical with one unpaired electron located in an in-plane orbital at the N atom (σ) and one at the *para*-C atom of the phenyl ring (σ), while the third unpaired electron is in an out-of-plane orbital of the N atom and is heavily delocalized into the π -system. Because of the significant delocalization of the out-of-plane SOMO, **Q-5** is expected to show both properties of a nitrene that is linked to a phenyl radical and of a carbene (cyclohexadienylidene) that is linked to a nitrogen-centered radical (iminy radical), as shown in the resonance structures below.



In accordance with this qualitative picture, the natural spin population³² is calculated to 1.55 unpaired electrons at the N atom and to 1.21 at the *para*-C atom (UB3LYP/TZVPP).

The closest related molecules to **Q-5** are a series of quartet-ground-state nitreno radicals **10**–**13** synthesized by Lahti et al.^{33–35}

(25) Zein, S.; Duboc, C.; Lubitz, W.; Neese, F. *Inorg. Chem.* **2007**, *47* (1), 134–142.

(26) Neese, F. *J. Chem. Phys.* **2007**, *127*, 164112.

(27) Duboc, C.; Phoeung, T.; Zein, S.; Pecaut, J.; Collomb, M. N.; Neese, F. *Inorg. Chem.* **2007**, *46*, 4905–4916.

(28) Carmieli, R.; Larsen, T. M.; Reed, G. H.; Zein, S.; Neese, F.; Goldfarb, D. *J. Am. Chem. Soc.* **2007**, *129*, 4240.

(29) Neese, F. *J. Inorg. Biochem.* **2006**, *100*, 716–726.

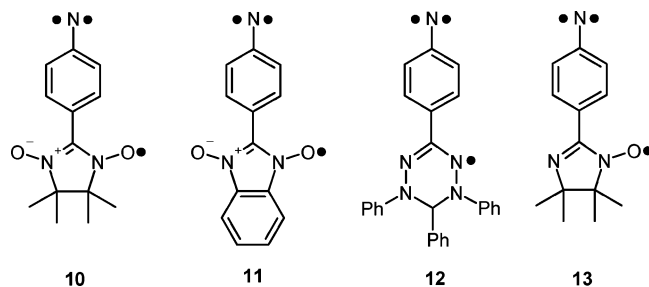
(30) Neese, F. *J. Am. Chem. Soc.* **2006**, *128*, 10213–10222.

(31) Schoneboom, J. C.; Neese, F.; Thiel, W. *J. Am. Chem. Soc.* **2005**, *127*, 5840–5853.

(32) Reed, A. E.; Weinstock, R. B.; Weinhold, F. *J. Chem. Phys.* **1985**, *83*, 1736.

(33) Lahti, P. M.; Esat, B.; Liao, Y.; Serwinski, P.; Lan, J.; Walton, R. *Polyhedron* **2001**, *20*, 1647–1652.

(34) Taylor, P.; Serwinski, P. R.; Lahti, P. M. *Org. Lett.* **2005**, *7*, 3693–3696.



The major difference from **5** is that, in **10–13**, a π -radical is attached to the phenylnitrene unit and, thus, the electronic structure is best-described as a σ,π,π -triradical. Consequently, a carbene-type resonance structure cannot be formulated for these molecules, which, in turn, has consequences for the ZFS parameter E (see below). The values for $|D/hc|$ of **10**, **11**, and **12** were determined to be 0.277, 0.256, and 0.288 cm^{-1} , respectively, which is similar to that of **5**, whereas $|E/hc|$ was found to be zero, contrary to that observed for **5**, which has a very large value of $|E/hc|$ (0.043). The quartet ground state of the para-connected triradicals **10–12** was rationalized in a spin fragment analysis by their nondisjointed nature favoring high-spin ground states.^{33,35} By contrast, the corresponding meta-connected systems prefer low-spin ground states. Only **13** has a doublet ground state with a reasonably small doublet–quartet splitting of 12 cal/mol, as determined by the analysis of the temperature dependence of the signal intensity (the Curie–Weiss plot).³⁴ The corresponding meta-connected system shows a larger preference for the doublet state, in accordance with the spin fragment analysis. In **13**, the ZFS parameters were determined to be $|D/hc| = 0.300$ and $|E/hc| = 0.0$ cm^{-1} , which indicates a higher spin density at the nitrene center and less delocalization of the nitrene π -electron. The value of D in nitreno radical **5** ($|D/hc| = 0.285$) is similar to that in **10** and **12**, which indicates a similar spin density at the nitrene center. However, the large E value in **5** deserves a closer interpretation.

In agreement with our calculations, Wasserman assumed that the direction of the principal magnetic axis z of phenyl nitrenes lies parallel to the N–C bond.^{5,36,37} It is readily verified (e.g., by a calculation on linear $^3\text{CH}_2$) that the dipolar field created by two unpaired electrons in p_x and p_y orbitals indeed points along the z -direction and that the axial symmetry of the spin distribution in such an arrangement remains untouched and leads to $|E/hc| = 0$. Indeed, for carbenes, it has been reported that the z -axis lies parallel to a hypothetical 180° bond angle,³⁸ and that the E value consequently increases with decreasing bond angle at the carbene center. The addition of a symmetrical π -radical in the para-position, as in **10–12**,³³ does not change the pseudo-cylindrical symmetry of these triradicals; the z -axis remains in the same position, and, hence, the E value of these quartet systems should remain zero.

However, this latter assumption cannot be verified. Our calculations demonstrate that the bulk of the E value results from one-center contributions of the direct spin–spin coupling interaction. This information, together with the fact that **Q-5**

simultaneously exhibits nitrene and carbene character, then leads to a simple and appealing geometric interpretation of the large value of E , in contrast to **10–13**, which have E values of zero. We assume, for **Q-5**, a coordinate system where the z -axis points along the C–N bond, the x -axis is perpendicular to the molecular plane, and the y -axis, consequently, lies in the molecular plane. In the nitrene part of the electronic structure, the two SOMOs are comprised of p_x and p_y orbitals and their dipolar field is consequently directed along the z -direction. For the carbene part of the 1^4A_2 ground state, the SOMOs are comprised of p_z and p_x contributions and, consequently, the resulting dipolar field points along the y -direction. Because the nitrene character prevails over the carbene character of **Q-5**, the main magnetic axis is still pointing along the C–N bond in the z -direction. However, the carbene character is reflected by an enhanced dipolar field in the y -direction, which is strong enough to give significantly magnetically inequivalent y - and x -directions. We, therefore, come to the conclusion that the nonzero E -value in **Q-5** mainly reflects the carbene character of the 1^4A_2 ground state. This carbene character, in turn, is controlled by the properties of the π -system, because the out-of-plane spin-density arises from the conjugation of the nitrene out-of-plane SOMO and the π -system of the ring.

Finally, the fact that the D value for **Q-5** is a factor of ~ 3 smaller than those of typical phenylnitrenes⁵ is readily explained by the prefactor $1/[S(2S - 1)]$ of the D^{SS} term (vide infra), which amounts to 1 for a ground state spin of 1 and $1/3$ for a ground-state spin of $3/2$. Assuming an axial D -tensor, the level splitting of $2D$ (in $S = 3/2$) versus D (in $S = 1$) is more similar for both multiplicities but is still slightly smaller for the quartet system. This is explained by the partial cancellation of the carbene and nitrene contributions to the D value, which oppose each other along the magnetic z -direction, as explained previously in some detail.

In summary, nitreno radical **Q-5** is an interesting σ,σ,π -triradical with unusual electronic and magnetic properties. The EPR spectrum could be completely analyzed and understood based on the qualitative and quantitative arguments. This makes it a benchmark system for understanding the organic quartet states. In addition, the robust quartet ground state makes this type of molecule interesting as models for new building blocks for the design of organic magnetic materials.

Experimental Section

Electron Paramagnetic Resonance (EPR) Measurements. X-band EPR spectra were recorded with a Bruker Model Elexsys E500 EPR spectrometer with a Model ER077R magnet (with a 75-mm gap between pole faces), a Model ER047 XG-T microwave bridge, and a Model ER4102ST resonator with a TE_{102} cavity. The matrices were deposited on an oxygen-free high-conductivity copper rod (75 mm in length, 3 mm in diameter) that was cooled by a Sumitomo SHI-4-5 closed-cycle 4.2 K cryostat. Because saturation of the spectra might be a problem, especially at 4 K, most spectra were recorded with a relatively high microwave power of 20.1 mW at 4 K and, in addition, with 0.64 mW at 15 K. The spectra were identical, only the signal-to-noise (s/n) ratio was much worse at higher temperature and lower power. Therefore, we assume that saturation is not significant under the experimental conditions used in our experiments.

The vacuum system consisted of a vacuum shroud that was equipped with a sample inlet valve and a half-closed quartz tube (75 mm in length, 10 mm in diameter) at the bottom and a vacuum pump system with a Pfeiffer Vacuum TMU071P turbo pump backed by a Leybold two-

(35) Serwinski, P. R.; Esat, B.; Lahti, P. M.; Liao, Y.; Walton, R.; Lan, J. *J. Org. Chem.* **2004**, *69*, 5247–5260.

(36) Smolinsky, G.; Wasserman, E.; Yager, W. A. *J. Am. Chem. Soc.* **1962**, *84*, 3220–3221.

(37) Smolinsky, G.; Snyder, L. C.; Wasserman, E. *Rev. Mod. Phys.* **1963**, *35*, 576–577.

(38) Wasserman, E.; Hutton, R. S. *Acc. Chem. Res.* **1977**, *10*, 27–32.

stage, rotary-vane pump. To avoid contamination of the high-vacuum segment by pump oil from the backing pump, a catalytic oxidation filter was placed between the rotary-vane pump and the turbo pump. During deposition, the inlet port was positioned at the same height as the tip of the copper rod. For irradiation, the copper rod was lowered into the quartz tube at the bottom of the shroud, and for the measurement of the EPR spectra, the entire apparatus was moved downward, so that the quartz tube and copper rod were positioned inside the EPR cavity.

Azide **6** was evaporated for 1 h at 0 °C and co-deposited with a large excess of argon (Messer–Griesheim, 99.9999%) on the tip of the copper rod at 4 K. The matrix-isolated sample was subsequently irradiated with a Lambda Physik Model Lextra 200 Excimer Laser (XeCl, 308 nm), and spectra were recorded at various irradiation times.

The computer simulation of the EPR spectrum was performed using the Xsophe computer simulation software suite (version 1.0.4),³⁹ which was developed by the Centre for Magnetic Resonance and Department of Mathematics, University of Queensland, Brisbane (Australia) and Bruker Analytik GmbH, Rheinstetten (Germany). The angular dependence of the quartet transitions was calculated using EasySpin.⁴⁰

EPR Calculations. The EPR properties were calculated according to previously published methods that are implemented in the ORCA package.^{24,26,30,41–47} Geometries were optimized using the BP86 functional,^{18,19} the TZVP basis set⁴⁸ (featuring a single set of polarization functions on each atom), and the resolution-of-the-identity approximation with matching auxiliary basis sets.^{49–51} Structures were verified to represent local minima through numeric frequency calculations.

Property calculations were done with the B3LYP hybrid functional, because, on average, it has been proven to be superior to nonhybrid functionals in EPR property calculations. In these calculations, a more extensively polarized triple- ζ basis set (TZVPP, amounting to 2d1f polarization shells all atoms) was used. The spin–spin (SS) contribution to the zero-field splitting tensor was treated in the mean-field approximation based on the Kohn–Sham determinant. The SS contribution is given by^{24,52,53}

$$D_{kl}^{(SS)} = -\frac{g_e^2}{16} \frac{\alpha^2}{S(2S-1)} \sum_{\mu\nu} \sum_{\kappa\tau} \times \{P_{\mu\nu}^{\alpha-\beta} P_{\kappa\tau}^{\alpha-\beta} - P_{\mu\kappa}^{\alpha-\beta} P_{\nu\tau}^{\alpha-\beta}\} \langle \mu\nu | r_{12}^{-5} \{3r_{12,k} r_{12,l} - \delta_{kl} r_{12}^2\} | \kappa\tau \rangle \quad (1)$$

- (39) Griffin, M.; Muys, A.; Noble, C.; Wang, D.; Eldershaw, C.; Gates, K. E.; Burrage, K.; Hanson, G. R. *Mol. Phys. Rep.* **1999**, *26*, 60–84.
 (40) Stoll, S.; Schweiger, A. *J. Magn. Reson.* **2006**, *178*, 42–55.
 (41) Neese, F.; Solomon, E. I. *Inorg. Chem.* **1998**, *37*, 6568–6582.
 (42) Neese, F. *J. Phys. Chem. A* **2001**, *105*, 4290–4299.
 (43) Neese, F. *J. Chem. Phys.* **2001**, *115*, 11080–11096.
 (44) Neese, F. *Curr. Opin. Chem. Biol.* **2003**, *7*, 125–135.
 (45) Neese, F. *J. Chem. Phys.* **2003**, *118*, 3939.
 (46) Neese, F. *J. Chem. Phys.* **2005**, *122*, 034107/034101–034113.
 (47) Neese, F. *J. Biol. Inorg. Chem.* **2006**, *11*, 702–711.
 (48) Schäfer, A.; Huber, C.; Ahlrichs, R. *J. Chem. Phys.* **1994**, *100*, 5829–5835.
 (49) Vahtras, O.; Almlöf, J.; Feyereisen, M. W. *Chem. Phys. Lett.* **1993**, *213*, 514–518.

Here, α is the fine structure constant ($\sim 1/137$ in atomic units); g_e is the free-electron g -value (2.002319...); the indices μ, ν, κ, τ refer to basis functions; and $P_{\mu\nu}^{\alpha-\beta}$ is an element of the spin-density matrix. No approximations have been made to the two-electron spin–spin dipole integrals in eq 1. As discussed previously,²⁴ it is advantageous to apply an open-shell spin-restricted formalism for this quantity, in conjunction with present-day DFT methods. We have used the spin densities from the spin-unrestricted natural orbital (UNO) determinant for this purpose, as discussed in detail in the work of Sinnecker and Neese.²⁴

Second-order SOC contributions also have been treated throughout the study. Following the general formulation, in terms of infinite sums over states,⁴¹ a linear response treatment was recently proposed in which the SOC contribution can be written as²⁶

$$D_{kl}^{(SOC;M)} = f_M(S) \langle \langle h_k^{SOC}; h_l^{SOC} \rangle \rangle \quad (2)$$

In eq 2, M denotes the contributions to the SOC term ($M = 0, \pm 1$) from excited states with $S' = S \pm 1$ (where S is the total spin quantum number of the electronic state for which the ZFS tensor is computed ($S > 1/2$)), $f_M(S)$ is a spin-dependent prefactor ($f_0 = -1/(4S^2)$, $f_{-1} = 1/[2S(2S-1)]$, $f_{+1} = 1/[2(S+1)(2S+1)]$), and $\langle \langle h_k^{SOC}; h_l^{SOC} \rangle \rangle$ is a shortcut notation for a spin–orbit linear response function. In a DFT framework, it is related to the derivatives of generalized spin densities, as explained in detail in ref 26. This treatment supersedes the earlier proposals for the SOC contribution to the ZFS tensor in the reports of Neese and co-workers^{54,55} and, in our opinion, also the work of Pederson and Khanna.⁵⁶ For alternative approaches, see the work of Reviakine et al.⁵⁷

The spin–orbit operator used in eq 2 was assumed to be of the spin–orbit mean-field (SOMF) type⁵⁸ in the multicenter implementation of Neese⁴⁶ that is equivalent to Berning et al.⁵⁹ It is believed to provide an accurate representation of the full Breit–Pauli two-electron SOC operator. The g -tensor has been calculated according to established procedures.^{43,46}

Acknowledgment. This work was financially supported by the Deutsche Forschungsgemeinschaft and the Fonds der Chemischen Industrie. F.N. and S.K. gratefully acknowledge the SFB 624 (“Template–vom Design chemischer Schablonen zur Reaktionssteuerung”, Universität Bonn) as well as the SFB 663 (“Molekulare Antwort nach elektronischer Anregung”, Universität Düsseldorf) for financial support.

JA078171S

- (50) Eichkorn, K.; Treutler, O.; Öhm, H.; Häser, M.; Ahlrichs, R. *Chem. Phys. Lett.* **1995**, *240*, 283–290.
 (51) Eichkorn, K.; Weigend, F.; Treutler, O.; Ahlrichs, R. *Theor. Chem. Acc.* **1997**, *97*, 119–124.
 (52) McWeeny, R.; Mizuno, Y. *Proc. R. Soc. (London)*, **A 1961**, A259, 554.
 (53) Petrenko, T. T.; Petrenko, T. L.; Bratus, V. Y. *J. Phys: Condens. Matter* **2002**, *14*, 12433–12440.
 (54) Ray, K.; Weyhermüller, T.; Neese, F.; Wiegardt, K. *Inorg. Chem.* **2005**, *44*, 5345–5360.
 (55) Pederson, M. R.; Khanna, S. N. *Phys. Rev. B* **1999**, *60*, 9566–9572.
 (56) Reviakine, R.; Arbuznikov, A. V.; Tremblay, J.-C.; Remenyi, C.; Malkina, O. L.; Malkin, V. G.; Kaupp, M. *J. Chem. Phys.* **2006**, *125*, 054110.
 (57) Hess, B. A.; Marian, C. M.; Wahlgren, U.; Gropen, O. *Chem. Phys. Lett.* **1996**, *251*, 365.
 (58) Berning, A.; Schweizer, M.; Werner, H. J.; Knowles, P. J.; Palmieri, P. *Mol. Phys.* **2000**, *98*, 1823–1833.
 (59) Pipek, J.; Mezey, P. G. *J. Chem. Phys.* **1989**, *90*, 4916–4926.